

## **AN ALTERNATIVE FORMULATION FOR GUIDED ELECTROMAGNETIC FIELDS IN GROUNDED CHIRAL SLABS**

J. C. da S. Lacava

Instituto Tecnológico de Aeronáutica  
Department of Electronic Engineering  
Praça Mal. Eduardo Gomes, 50  
12228-900 São José dos Campos, SP - Brazil

F. Lumini

EMBRAER S. A.  
Division of Systems Engineering  
Av. Brig. Faria Lima, 2170  
12227-901 São José dos Campos, SP - Brazil

- 1. Introduction**
  - 2. The Geometry of the Problem**
  - 3. Electromagnetic Fields in Region 1**
  - 4. Electromagnetic Fields in Region 2**
  - 5. Boundary Conditions and Dispersion Equation**
  - 6. Expressions for Guided Electromagnetic Fields**
  - 7. Numerical Results**
  - 8. Conclusions**
- Acknowledgments**  
**References**

### **1. INTRODUCTION**

Open chirostrip structures consist of conventional microstrip devices in which the dielectric substrate is replaced by a slab of chiral material. This class of structures has gained considerable attention due to the possibility of fabricating such material in the microwave and millimeter-wave frequency ranges. Its potential applications in future

designs of new devices and components have been emphasized by several authors [1]. Because of this, important canonical problems involving chirostrip structures have been analyzed. Effects of the chiral admittance on radiation patterns, input impedance, near field distributions and crosspolarization level have been studied and reported in the technical literature. Patch antennas, dipoles and infinite arrays printed on grounded chiral slabs have been analyzed [2–8]. Electromagnetic properties of guided modes in chirowaveguides are another topic of interest. Recently, Mariotte, Pelet, and Engheta presented an excellent review of this subject [9]. The special case of surface wave modes in grounded chiral slabs has also been discussed [3,9–11].

The purpose of this work is to present an alternative formulation for the analysis of guided electromagnetic fields in grounded chiral slabs. Although in a rather different context, this formulation is formally equivalent to that used by the authors to calculate the spectral fields in open chirostrip structures [5,8,12,13]. Furthermore, effects of chirality on electromagnetic field distributions and on dispersion curves of surface wave modes are also analyzed. It has been observed that, inside a chiral substrate and at the interface with a perfectly conducting surface, the magnetic field component normal to this surface is not null. Moreover, at the interface between a chiral substrate and the free space, the magnetic field component normal to this interface is not continuous even when the magnetic permeability is the same in the two media.

## 2. THE GEOMETRY OF THE PROBLEM

Fig. 1 shows the geometry of a grounded chiral slab. A homogeneous isotropic linear chiral substrate of thickness  $d$ , permittivity  $\varepsilon$ , permeability  $\mu$  and chiral admittance  $\xi$ , lies on an infinite perfectly conducting plate, located on the  $x$ - $y$  plane of a rectangular coordinate system. The planar interface  $z = d$  separates the chiral medium (region 1:  $0 < z < d$ ) from the free space region (region 2:  $z > d$ , permittivity  $\varepsilon_0$  and permeability  $\mu_0$ ). For lossless chiral substrates, the parameters  $\varepsilon$ ,  $\mu$  and  $\xi$  are real quantities.

In our formulation, expressions for guided electromagnetic fields are obtained from the solution of the wave equations in regions 1 and 2. After that, the boundary conditions for the electromagnetic fields are applied on the interfaces  $z = 0$  and  $z = d$ . This allows the unique determination of the electromagnetic field distributions at any point

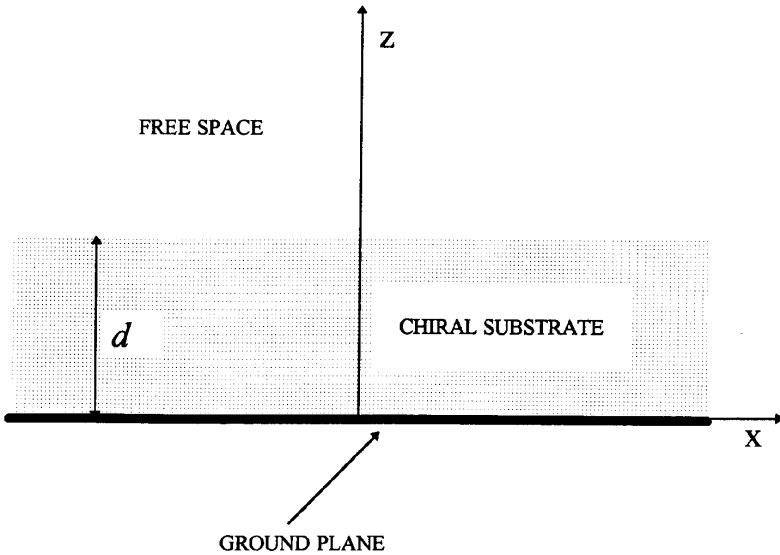


**Figure 1.** Geometry of a grounded chiral slab.

in the region  $z > 0$ , which can be expressed in simple closed forms. The dispersion equation for surface wave modes is also derived.

### 3. ELECTROMAGNETIC FIELDS IN REGION 1

In this section, expressions for guided electromagnetic fields inside the chiral substrate ( $0 < z < d$ ) are derived. For time harmonic variations, assuming time dependence of the form  $e^{i\omega t}$ , Maxwell equations for source-free media are given by

$$\nabla \times \vec{\mathbf{E}} = -i\omega\vec{\mathbf{B}} \tag{1}$$

$$\nabla \times \vec{\mathbf{H}} = i\omega\vec{\mathbf{D}} \tag{2}$$

$$\nabla \cdot \vec{\mathbf{D}} = 0 \tag{3}$$

$$\nabla \cdot \vec{\mathbf{B}} = 0 \tag{4}$$

Using the Post-Jaggard time-harmonic constitutive relations for isotropic reciprocal chiral media [14],

$$\vec{\mathbf{D}} = \epsilon\vec{\mathbf{E}} - i\xi\vec{\mathbf{B}} \tag{5}$$

$$\vec{\mathbf{B}} = \mu\vec{\mathbf{H}} + i\mu\xi\vec{\mathbf{E}} \tag{6}$$

the wave equations for electromagnetic fields inside the substrate can be written as

$$\nabla^2 \vec{\mathbf{E}} + 2p \nabla \times \vec{\mathbf{E}} + k^2 \vec{\mathbf{E}} = 0 \quad (7)$$

$$\nabla^2 \vec{\mathbf{H}} + 2p \nabla \times \vec{\mathbf{H}} + k^2 \vec{\mathbf{H}} = 0 \quad (8)$$

where

$$k^2 = \omega^2 \mu \varepsilon \quad (9)$$

$$p = \omega \mu \xi \quad (10)$$

As the geometry shown in Fig. 1 is unbounded in the  $x$  and  $y$  directions, and the chiral substrate is a linear homogeneous medium, we can assume without loss of generality that the surface waves propagate along the  $x$  direction. Hence, we propose the following vector functions for the electric and magnetic fields, inside the chiral substrate:

$$\vec{\mathbf{E}}(x, z) = \vec{\mathcal{E}}(z) e^{-i\beta x} \quad (11)$$

$$\vec{\mathbf{H}}(x, z) = \vec{\mathcal{H}}(z) e^{-i\beta x} \quad (12)$$

where  $\beta$ , the propagation constant along the  $x$  direction, is a real and positive quantity in the lossless case.

Introducing expression (11) into the wave equation (7), we obtain the following fourth order differential equation:

$$\frac{d^4 \mathcal{E}_\eta(z)}{dz^4} + 2(k^2 - \beta^2 + 2p^2) \frac{d^2 \mathcal{E}_\eta(z)}{dz^2} + (\beta^4 - 4p^2 \beta^2 - 2k^2 \beta^2 + k^4) \mathcal{E}_\eta(z) = 0 \quad (13)$$

where  $\eta = x, y$  or  $z$ .

Assuming solutions expressed in the form

$$\mathcal{E}_\eta(z) = \mathbf{e}_\eta e^{i\gamma z} \quad (14)$$

where  $\mathbf{e}_\eta$  are constants to be determined, the following biquadratic equation can be obtained:

$$\gamma^4 - 2(k^2 - \beta^2 + 2p^2)\gamma^2 + (\beta^4 - 4p^2 \beta^2 - 2k^2 \beta^2 + k^4) = 0 \quad (15)$$

Solving this equation, four different propagation constants in the  $z$  direction are determined. In our work, these propagation constants are expressed as

$$\gamma_1 = -\gamma_3 = \sqrt{k_+^2 - \beta^2} \quad (16)$$

$$\gamma_2 = -\gamma_4 = \sqrt{k_-^2 - \beta^2} \quad (17)$$

where  $k_+ = q + p$ ,  $k_- = q - p$  and  $q = (k^2 + p^2)^{1/2}$ . According to [2],  $k_+$  and  $k_-$  are the wave numbers of the right and left-circularly polarized waves propagating in an unbounded chiral medium.

Introducing (14) in (11) we can write the expressions for the electric field components inside the chiral substrate in the following way

$$\mathbf{E}_\eta(x, z) = \left\{ \sum_{\tau=1}^4 \mathbf{e}_{\eta\tau} e^{i\gamma_\tau z} \right\} e^{-i\beta x} \quad (18)$$

Using similar development, the components of the magnetic field are given by

$$\mathbf{H}_\eta(x, z) = \left\{ \sum_{\tau=1}^4 \mathbf{h}_{\eta\tau} e^{i\gamma_\tau z} \right\} e^{-i\beta x} \quad (19)$$

At this time we have twenty five unknowns: the constants  $\mathbf{e}_{\eta\tau}$  and  $\mathbf{h}_{\eta\tau}$  ( $\eta = x, y$  or  $z$ ;  $\tau = 1, 2, 3$  or  $4$ ) and the propagation constant  $\beta$ .

Introducing expressions (18) and (19) in the Maxwell equations (1) and (2), the following relations involving  $\mathbf{e}_{\eta\tau}$  and  $\mathbf{h}_{\eta\tau}$  are obtained

$$\mathbf{e}_{x\tau} = \frac{\gamma_\tau}{\beta} \mathbf{e}_{z\tau} \quad (20)$$

$$\mathbf{e}_{y\tau} = (-1)^{\tau+1} \frac{ik_\tau}{\beta} \mathbf{e}_{z\tau} \quad (21)$$

$$\mathbf{h}_{x\tau} = (-1)^{\tau+1} \frac{i\gamma_\tau}{\beta\eta_c} \mathbf{e}_{z\tau} \quad (22)$$

$$\mathbf{h}_{y\tau} = -\frac{k_\tau}{\beta\eta_c} \mathbf{e}_{z\tau} \quad (23)$$

$$\mathbf{h}_{z\tau} = (-1)^{\tau+1} \frac{i}{\eta_c} \mathbf{e}_{z\tau} \quad (24)$$

where  $k_1 = k_3 = k_+$ ,  $k_2 = k_4 = k_-$ ,  $\eta_c = (\mu/\epsilon_c)^{1/2}$  is the intrinsic impedance of the chiral medium and  $\epsilon_c = \epsilon + \mu\xi^2$  its equivalent permittivity. With this procedure, we have drastically reduced the number of the unknowns in the chiral substrate. They are now only the propagation constant  $\beta$  and the constants  $\mathbf{e}_{z1}$ ,  $\mathbf{e}_{z2}$ ,  $\mathbf{e}_{z3}$  and  $\mathbf{e}_{z4}$ .

#### 4. ELECTROMAGNETIC FIELDS IN REGION 2

The wave equations for the electromagnetic fields in the free space ( $z > d$ ) can be obtained from equations (7) and (8) if the particular

conditions  $\xi = 0$ ,  $\varepsilon = \varepsilon_0$  and  $\mu = \mu_0$  are observed. After the substitution of these values, we have

$$\nabla^2 \vec{\mathbf{E}}_0 + k_0^2 \vec{\mathbf{E}}_0 = 0 \quad (25)$$

$$\nabla^2 \vec{\mathbf{H}}_0 + k_0^2 \vec{\mathbf{H}}_0 = 0 \quad (26)$$

where

$$k_0^2 = \omega^2 \mu_0 \varepsilon_0 \quad (27)$$

Using a procedure similar to that presented in the previous section, the expressions for the electromagnetic field components in the free space region are given by

$$\mathbf{E}_{\eta 0}(x, z) = \mathbf{e}_{\eta 0} e^{-(\alpha z + i\beta x)} \quad (28)$$

$$\mathbf{H}_{\eta 0}(x, z) = \mathbf{h}_{\eta 0} e^{-(\alpha z + i\beta x)} \quad (29)$$

where  $\alpha$  is the attenuation rate in the  $z$  direction of the guided modes, a real and positive quantity, and is written as:

$$\alpha = \sqrt{\beta^2 - k_0^2} \quad (30)$$

In the free space region, the constants  $\mathbf{e}_{\eta 0}$  and  $\mathbf{h}_{\eta 0}$  satisfy the following relations

$$\mathbf{e}_{x0} = \frac{i\alpha}{\beta} \mathbf{e}_{z0} \quad (31)$$

$$\mathbf{e}_{y0} = \frac{\omega\mu_0}{\beta} \mathbf{h}_{z0} \quad (32)$$

$$\mathbf{h}_{x0} = \frac{i\alpha}{\beta} \mathbf{h}_{z0} \quad (33)$$

$$\mathbf{h}_{y0} = -\frac{\omega\varepsilon_0}{\beta} \mathbf{e}_{z0} \quad (34)$$

After that, besides the propagation constant  $\beta$ , only the constants  $\mathbf{e}_{z0}$  and  $\mathbf{h}_{z0}$  are unknown in this region.

## 5. BOUNDARY CONDITIONS AND DISPERSION EQUATION

For the grounded chiral slab presented in Fig. 1, the necessary and sufficient boundary conditions are those that require the tangential

components of the electric field to vanish on the ground plane ( $z = 0$ ) and the continuity of the tangential components of the electric and magnetic fields on the chiral-free space interface  $z = d$ . After the application of these conditions, we can write the following system of equations involving  $\mathbf{e}_{z\tau}$ ,  $\mathbf{e}_{z0}$  and  $\mathbf{h}_{z0}$ :

$$\sum_{\tau=1}^4 (\gamma_{\tau} \mathbf{e}_{z\tau}) = 0 \quad (35)$$

$$\sum_{\tau=1}^4 [(-1)^{\tau+1} k_{\tau} \mathbf{e}_{z\tau}] = 0 \quad (36)$$

$$\sum_{\tau=1}^4 [\gamma_{\tau} e^{i\gamma_{\tau} d} \mathbf{e}_{z\tau}] = i\alpha e^{-\alpha d} \mathbf{e}_{z0} \quad (37)$$

$$\sum_{\tau=1}^4 [(-1)^{\tau+1} k_{\tau} e^{i\gamma_{\tau} d} \mathbf{e}_{z\tau}] = -i\omega\mu_0 e^{-\alpha d} \mathbf{h}_{z0} \quad (38)$$

$$\sum_{\tau=1}^4 \left[ (-1)^{\tau+1} \frac{\gamma_{\tau}}{\eta_c} e^{i\gamma_{\tau} d} \mathbf{e}_{z\tau} \right] = \alpha e^{-\alpha d} \mathbf{h}_{z0} \quad (39)$$

$$\sum_{\tau=1}^4 \left[ \frac{k_{\tau}}{\eta_c} e^{i\gamma_{\tau} d} \mathbf{e}_{z\tau} \right] = \omega\epsilon_0 e^{-\alpha d} \mathbf{e}_{z0} \quad (40)$$

In order to have a solution different from zero for the system (35)–(40), we must force its determinant to be zero. This results in the following dispersion equation for surface wave modes, guided in the chiral substrate:

$$\begin{aligned} & \eta_c \gamma_2 k_- (\gamma_1^2 k_0^2 - \alpha^2 k_+^2) \sin(\gamma_1 d) \cos(\gamma_2 d) \\ & - \alpha \omega \gamma_1 \gamma_2 k^2 (\epsilon_0 \eta_c^2 + \mu_0) \cos(\gamma_1 d) \cos(\gamma_2 d) \\ & + 0.5 \alpha \omega (\gamma_1^2 k_-^2 + \gamma_2^2 k_+^2) (\epsilon_0 \eta_c^2 + \mu_0) \sin(\gamma_1 d) \sin(\gamma_2 d) \\ & + \eta_c \gamma_1 k_+ (\gamma_2^2 k_0^2 - \alpha^2 k_-^2) \cos(\gamma_1 d) \sin(\gamma_2 d) \\ & + \alpha \omega \gamma_1 \gamma_2 k^2 (\epsilon_0 \eta_c^2 - \mu_0) = 0 \end{aligned} \quad (41)$$

According to [15], the cut-off frequencies of these modes are found by setting  $\alpha = 0$  in (41). When this is done, we get the following equation:

$$k_- \gamma_{1c} \sin(\gamma_{1c} d) \cos(\gamma_{2c} d) + k_+ \gamma_{2c} \sin(\gamma_{2c} d) \cos(\gamma_{1c} d) = 0 \quad (42)$$

where

$$\gamma_{1c} = (k_+^2 - k_0^2)^{1/2} \quad (43)$$

$$\gamma_{2c} = (k_-^2 - k_0^2)^{1/2} \quad (44)$$

Equations (41) and (42) are similar to the equations for dispersion curves and cut-off frequencies presented in [3, 11]. In an achiral slab (i.e., for  $\xi = 0.0\text{S}$ ), (41) and (42) reduce to the standard equations for TE and TM guided modes [15].

We observe that  $k_0$  is the lowest value for the propagation constant of any guided mode because, if  $\beta$  were less than  $k_0$ ,  $\alpha$  would be purely imaginary and the fields in the free space region would be proportional to  $e^{-iz(k_0^2 - \beta^2)^{1/2}}$ . In this case, we would get the so called radiation modes and the structure behaves like a leaky-wave antenna. On the other hand, analyzing (41) we note that, under the condition  $\beta < k_0$ , this expression is complex and it is not possible to find a  $\beta$  that simultaneously sets to zero its real and imaginary parts.

We also observe that  $k_+$  is the highest value for the propagation constant of any guided mode because, if  $\beta$  were greater than  $k_+$ ,  $\gamma_1$  and  $\gamma_2$  would be purely imaginary. This means that all modes associated to these propagation constants would be attenuated. It can also be observed that, when  $\beta$  is greater than  $k_+$ , (41) is negative, purely imaginary and cannot be zeroed.

As pointed out in [3], guided waves in grounded chiral slabs are possible if the condition  $k_+ > \beta > k_0$  is satisfied.

## 6. EXPRESSIONS FOR GUIDED ELECTROMAGNETIC FIELDS

Solutions of the dispersion equation (41) and of the system (35)–(40) yield the propagation constant  $\beta$  of a given guided mode and the expressions for  $\mathbf{e}_{z\tau}$ ,  $\mathbf{e}_{z0}$  and  $\mathbf{h}_{z0}$ . Substituting the values obtained for  $\beta$ ,  $\mathbf{e}_{z\tau}$ ,  $\mathbf{e}_{z0}$  and  $\mathbf{h}_{z0}$  into equations (20)–(24) and (31)–(34) and then into equations (18), (19), (28) and (29), we obtain the following expressions for the components of the electric and magnetic fields of guided modes, inside and outside the chiral substrate:

a) Inside the chiral substrate ( $0 < z < d$ )

$$\mathbf{E}_x(x, z) = \frac{2i\mathbf{e}_{z4}}{\beta\Delta} \left\{ \gamma_1\gamma_2[\cos(\gamma_1z) - \cos(\gamma_2z)]W_1 + [\gamma_1k_- \sin(\gamma_1z) + \gamma_2k_+ \sin(\gamma_2z)]W_2 \right\} e^{-i\beta x} \quad (45)$$

$$\mathbf{E}_y(x, z) = \frac{2i\mathbf{e}_{z4}}{\beta\Delta} \left\{ k^2[\cos(\gamma_1z) - \cos(\gamma_2z)]W_2 - [\gamma_2k_+ \sin(\gamma_1z) + \gamma_1k_- \sin(\gamma_2z)]W_1 \right\} e^{-i\beta x} \quad (46)$$

$$\mathbf{E}_z(x, z) = \frac{2\mathbf{e}_{z4}}{\Delta} \left\{ [k_- \cos(\gamma_1z) + k_+ \cos(\gamma_2z)]W_2 - [\gamma_2 \sin(\gamma_1z) - \gamma_1 \sin(\gamma_2z)]W_1 \right\} e^{-i\beta x} \quad (47)$$

$$\mathbf{H}_x(x, z) = -\frac{2\mathbf{e}_{z4}}{\beta\Delta\eta_c} \left\{ \gamma_1\gamma_2[\cos(\gamma_1z) + \cos(\gamma_2z)]W_1 + [\gamma_1k_- \sin(\gamma_1z) - \gamma_2k_+ \sin(\gamma_2z)]W_2 \right\} e^{-i\beta x} \quad (48)$$

$$\mathbf{H}_y(x, z) = -\frac{2\mathbf{e}_{z4}}{\beta\Delta\eta_c} \left\{ k^2[\cos(\gamma_1z) + \cos(\gamma_2z)]W_2 - [\gamma_2k_+ \sin(\gamma_1z) - \gamma_1k_- \sin(\gamma_2z)]W_1 \right\} e^{-i\beta x} \quad (49)$$

$$\mathbf{H}_z(x, z) = \frac{2i\mathbf{e}_{z4}}{\Delta\eta_c} \left\{ [k_- \cos(\gamma_1z) - k_+ \cos(\gamma_2z)]W_2 - [\gamma_2 \sin(\gamma_1z) + \gamma_1 \sin(\gamma_2z)]W_1 \right\} e^{-i\beta x} \quad (50)$$

where

$$\Delta = (\gamma_1\gamma_2k_+k_- + i\alpha\gamma_1k_-^2) \cos(\gamma_1d) - i(\gamma_1^2k_+k_- + i\alpha\gamma_2k_+^2) \sin(\gamma_1d) - (\gamma_1\gamma_2k_+k_- - i\alpha\gamma_1k_-^2) e^{i\gamma_2d} \quad (51)$$

$$k_a = \omega\varepsilon_0\eta_c \quad (52)$$

$$W_1 = \alpha k^2[\cos(\gamma_1d) + \cos(\gamma_2d)] - k_a[\gamma_1k_- \sin(\gamma_1d) + \gamma_2k_+ \sin(\gamma_2d)] \quad (53)$$

$$W_2 = \gamma_1\gamma_2k_a[\cos(\gamma_1d) - \cos(\gamma_2d)] + \alpha[\gamma_2k_+ \sin(\gamma_1d) - \gamma_1k_- \sin(\gamma_2d)] \quad (54)$$

b) Outside the chiral substrate ( $z > d$ )

$$\mathbf{E}_{x0}(x, z) = \frac{2i\alpha\mathbf{e}_{z4}}{\beta\Delta} Y_1 e^{[\alpha(d-z) - i\beta x]} \quad (55)$$

$$\mathbf{E}_{y0}(x, z) = \frac{2i\mathbf{e}_{z4}}{\beta\Delta} Y_2 e^{[\alpha(d-z)-i\beta x]} \quad (56)$$

$$\mathbf{E}_{z0}(x, z) = \frac{2\mathbf{e}_{z4}}{\Delta} Y_1 e^{[\alpha(d-z)-i\beta x]} \quad (57)$$

$$\mathbf{H}_{x0}(x, z) = -\frac{2\alpha\mathbf{e}_{z4}}{\omega\beta\Delta\mu_0} Y_2 e^{[\alpha(d-z)-i\beta x]} \quad (58)$$

$$\mathbf{H}_{y0}(x, z) = -\frac{2\omega\varepsilon_0\mathbf{e}_{z4}}{\beta\Delta} Y_1 e^{[\alpha(d-z)-i\beta x]} \quad (59)$$

$$\mathbf{H}_{z0}(x, z) = \frac{2i\mathbf{e}_{z4}}{\omega\Delta\mu_0} Y_2 e^{[\alpha(d-z)-i\beta x]} \quad (60)$$

where

$$Y_1 = (\gamma_2^2 k_+^2 - \gamma_1^2 k_-^2) \sin(\gamma_1 d) \sin(\gamma_2 d) \quad (61)$$

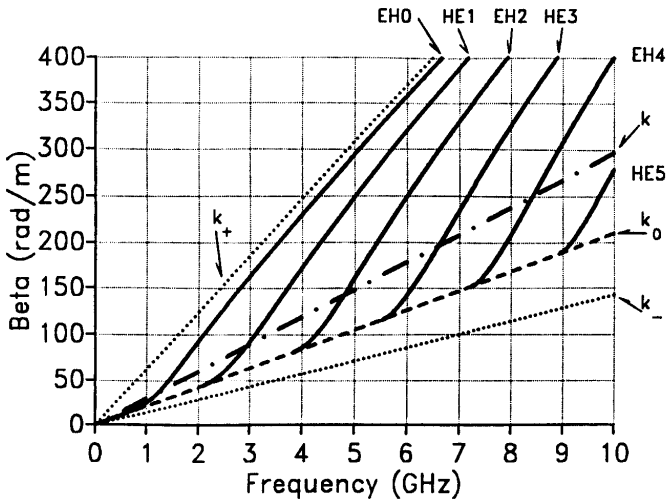
$$Y_2 = 2\gamma_1\gamma_2 k_a k^2 [1 - \cos(\gamma_1 d) \cos(\gamma_2 d)] - 2\alpha k^2 [\gamma_1 k_- \cos(\gamma_1 d) \sin(\gamma_2 d) + \gamma_2 k_+ \sin(\gamma_1 d) \cos(\gamma_2 d)] + k_a (\gamma_2^2 k_+^2 + \gamma_1^2 k_-^2) \sin(\gamma_1 d) \sin(\gamma_2 d) \quad (62)$$

It is worth pointing out that, in our approach, we have considered  $\mathbf{e}_{z4}$  as a parameter depending on the excitation.

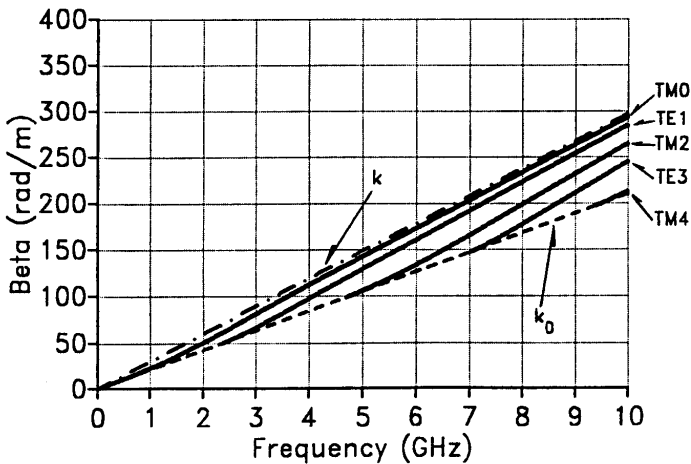
## 7. NUMERICAL RESULTS

Using the formulation described above, effects of chirality on electromagnetic field distributions and on dispersion curves of several surface wave modes were analyzed. We have chosen chiral admittance values normally found in the literature [1, 16] and, for brevity, only the results for the chirostrip structure with  $\varepsilon = 2.0\varepsilon_0$ ,  $\mu = \mu_0$ , and  $d = 32.0$  mm are discussed below.

Dispersion curves for  $\xi = 3.0$  mS and for  $\xi = 0.0$  S (achiral substrate) are presented in Figs. 2(A) and 2(B), respectively. In Fig. 2(A) the dashed line corresponds to the geometric locus of  $k_0$ , the upper dotted line corresponds to the geometric locus of  $k_+$ , the lower one to the geometric locus of  $k_-$  and the dot-dash line corresponds to the geometric locus of  $k$ . When the substrate is achiral (Fig. 2(B)), the geometric loci of  $k_+$  and  $k_-$  coincide with that of  $k$ . In Figs. 2(A) and 2(B) we note that, increasing the chirality parameter,  $k_+$  moves away from  $k$  upward and  $k_-$  downward. This occurs because the relation  $k_+ k_- = k^2$  is valid for any  $\xi$ . It is worth noting that, when  $\xi > (\varepsilon_r - 1)/(2\eta_0)$ , where  $\eta_0$  is the intrinsic impedance of the free



(A)



(B)

**Figure 2.** Dispersion curves for guided modes with  $d = 32.0$  mm,  $\mu = \mu_0$  and  $\epsilon = 2.0\epsilon_0$ . (A)  $\xi = 3.0$  mS; (B) achiral substrate.

space and  $\varepsilon_r = \varepsilon/\varepsilon_0$ , we have  $k_- < k_0$ . Considering the chiral substrate constitutive parameters used in these examples, the inequality  $k_- < k_0$  occurs when  $\xi$  is greater than 1.33 mS. This situation can be observed in Fig. 2(A) for  $\xi = 3.0$  mS. As we pointed out in Section 5, all dispersion curves are located between the  $k_0$  and  $k_+$  curves. We observe in Figs. 2(A) and 2(B) that the first mode of propagation has no cut-off frequency. We also observe that chirality tends to increase the number of propagating modes for a given operating frequency. For example, at 6.0 GHz the achiral substrate supports three different propagating modes:  $\text{TM}_0$ ,  $\text{TE}_1$  and  $\text{TM}_2$ . When chirality increases to 3.0 mS, this number increases to four hybrid propagating modes:  $\text{EH}_0$ ,  $\text{HE}_1$ ,  $\text{EH}_2$  and  $\text{HE}_3$ .

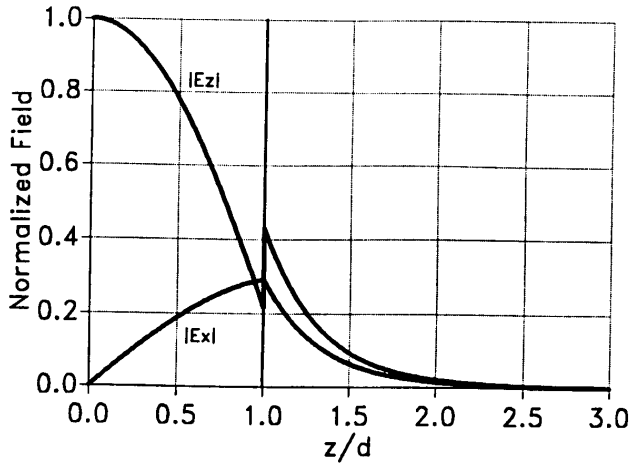
Effects of chirality on field patterns for the first and the second propagating modes will now be discussed. In all cases, we employ the frequency of 5.0 GHz. In Figs. 3 and 4 we have drawn the magnitudes of the electric and magnetic fields for the first propagating mode. Figs. 3(A) and 4(A) were plotted for an achiral substrate ( $\text{TM}_0$  mode) and Figs. 3(B) and 4(B) for  $\xi = 0.1$  mS ( $\text{EH}_0$  mode). As expected, the components  $\mathbf{E}_y$ ,  $\mathbf{H}_x$  and  $\mathbf{H}_z$  are not present in the  $\text{TM}_0$  mode but appear with the chirality in the hybrid  $\text{EH}_0$  mode.

Field patterns for the second propagating mode were plotted in Figs. 5 and 6. When the substrate is achiral, only the  $\mathbf{E}_y$ ,  $\mathbf{H}_x$  and  $\mathbf{H}_z$  components are present, and the propagating mode is the  $\text{TE}_1$ . On the other hand, increasing the chirality, all the components are present and, in this case, the chiral substrate supports the hybrid  $\text{HE}_1$  propagating mode.

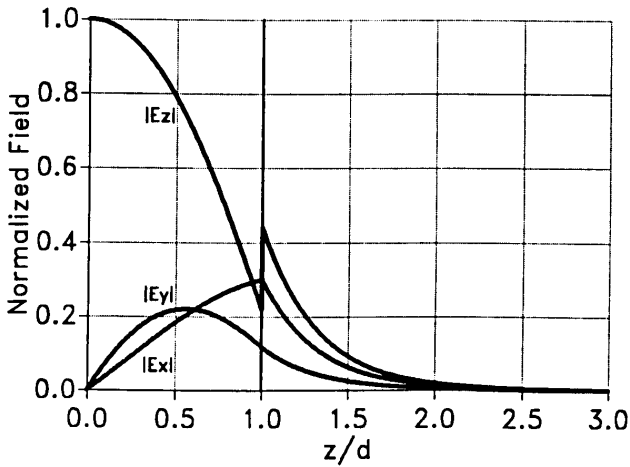
Finally, in Figs. 7(A) and 7(B), we have drawn the amplitudes of  $|\mathbf{H}_z|$  and  $|\mathbf{B}_z|$  versus  $z/d$  for the first hybrid mode and  $\xi = 1.0$  mS to better observe their behavior at  $z = d$  and  $z = 0$ . Two interesting things related to the magnetic field component  $\mathbf{H}_z$  can be observed in Fig. 7(A):

- a) the magnetic field component normal to a perfectly conducting surface is not zero in a chiral medium. It can be shown analytically that the value of the  $\mathbf{H}_z$  component at  $z = 0$  interface is given by

$$H_z(x, 0) = -\frac{4i\omega\mu_0 W_2 e^{-i\beta x} \mathbf{e}_{z4}}{\Delta\eta_c} \xi \quad (63)$$

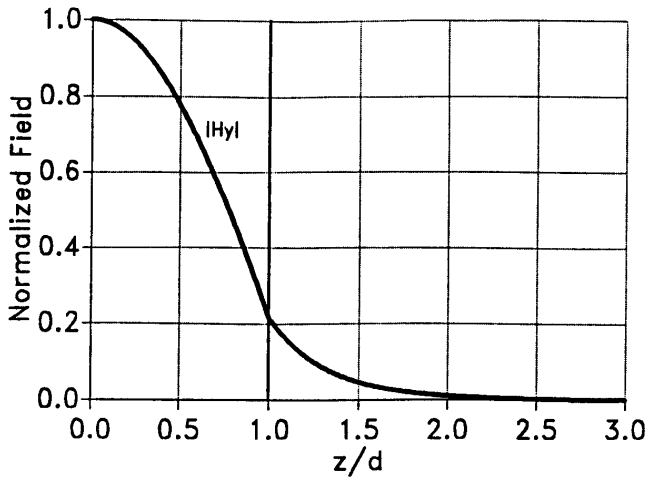


(A)

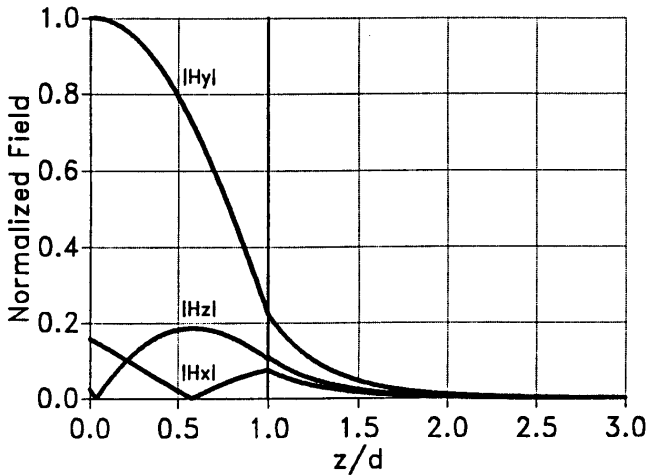


(B)

**Figure 3.** Electric field patterns for the first propagating mode with  $d = 32.0$  mm,  $\mu = \mu_0$ ,  $\varepsilon = 2.0\varepsilon_0$  and  $f = 5.0$  GHz. (A) achiral substrate ( $TM_0$  mode); (B)  $\xi = 0.1$  mS ( $EH_0$  mode).

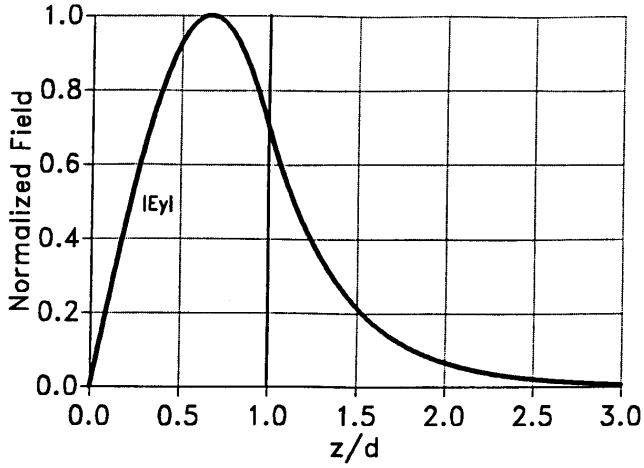


(A)

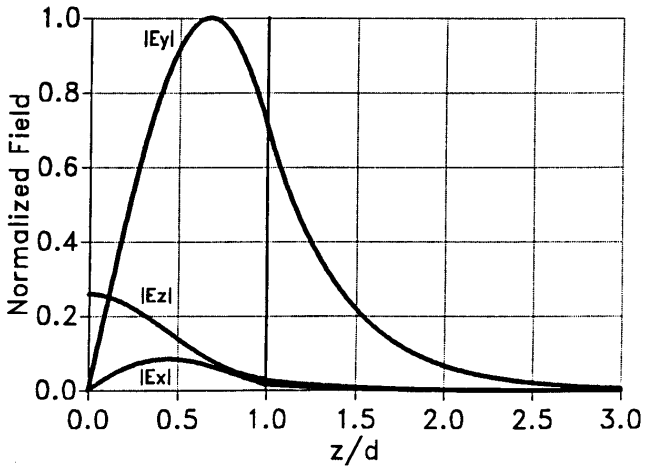


(B)

**Figure 4.** Magnetic field patterns for the first propagating mode with  $d = 32.0$  mm,  $\mu = \mu_0$ ,  $\varepsilon = 2.0\varepsilon_0$  and  $f = 5.0$  GHz. (A) achiral substrate ( $TM_0$  mode); (B)  $\xi = 0.1$  mS ( $EH_0$  mode).

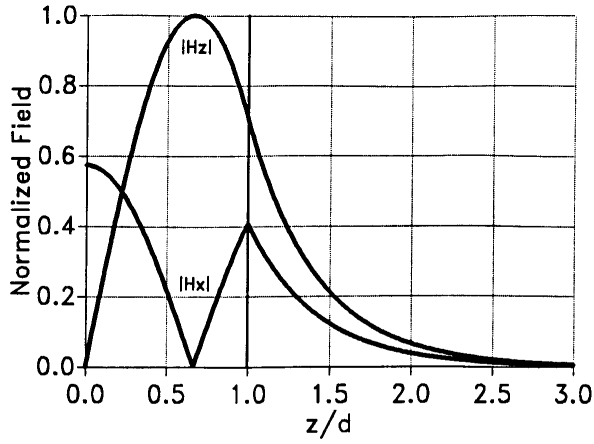


(A)

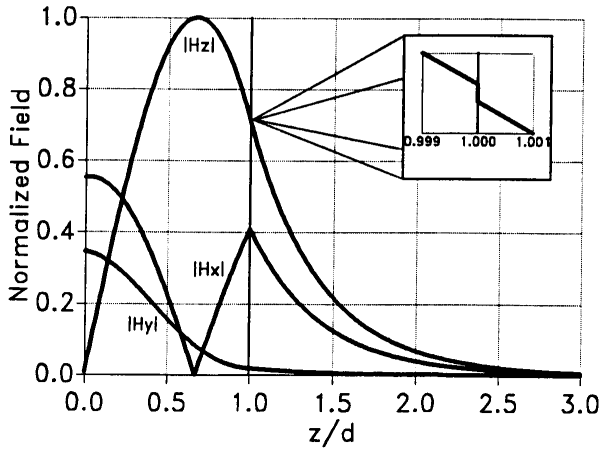


(B)

**Figure 5.** Electric field patterns for the second propagating mode with  $d = 32.0$  mm,  $\mu = \mu_0$ ,  $\varepsilon = 2.0\varepsilon_0$  and  $f = 5.0$  GHz. (A) achiral substrate ( $TE_1$  mode); (B)  $\xi = 0.1$  mS ( $HE_1$  mode).

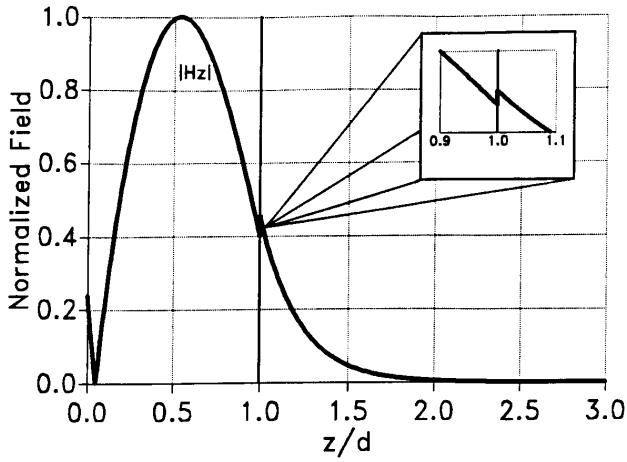


(A)

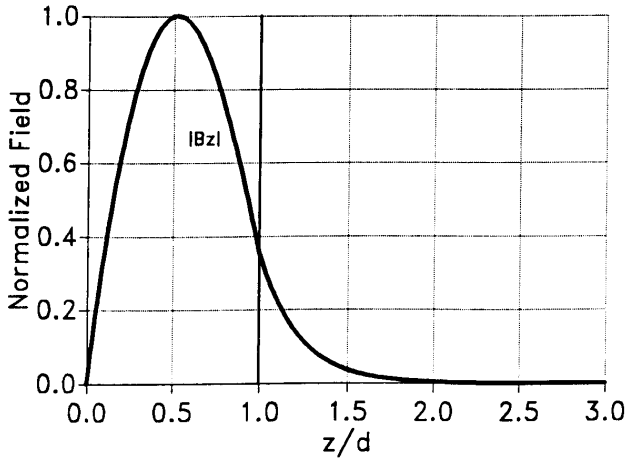


(B)

**Figure 6.** Magnetic field patterns for the second propagating mode with  $d = 32.0$  mm,  $\mu = \mu_0$ ,  $\varepsilon = 2.0\varepsilon_0$  and  $f = 5.0$  GHz. (A) achiral substrate ( $TE_1$  mode); (B)  $\xi = 0.1$  mS ( $HE_1$  mode). The region between  $z = 0.999d$  and  $z = 1.001d$  has been expanded to show the discontinuity in the  $|\mathbf{H}_z|$  component.



(A)



(B)

**Figure 7.** Magnitudes of  $\mathbf{H}_z$  and  $\mathbf{B}_z$  versus  $z/d$  with  $\xi = 1.0 \text{ mS}$ , for the first hybrid mode. The region from  $z = 0.9d$  to  $z = 1.1d$  has been expanded to show the discontinuity in the  $|\mathbf{H}_z|$  component.

- b)  $\mathbf{H}_z$  is not continuous on the interface between the chiral substrate and the free space region even when the permeability is the same in the two media. The difference between  $\mathbf{H}_z(x, d)$  and  $\mathbf{H}_{z0}(x, d)$  can be expressed as:

$$\begin{aligned} \mathbf{H}_z(x, d) - \mathbf{H}_{z0}(x, d) = & \\ & \frac{4i\gamma_1\gamma_2\omega\mu_0e^{-i\beta x}\mathbf{e}_{z4}}{\Delta} \left\{ k_a[1 - \cos(\gamma_1 d)\cos(\gamma_2 d)] \right. \\ & - \alpha d[k_+ \cos(\gamma_2 d)\text{sinc}(\gamma_1 d) + k_- \cos(\gamma_1 d)\text{sinc}(\gamma_2 d)] \\ & \left. + k_a d^2(k^2 + \beta^2)\text{sinc}(\gamma_1 d)\text{sinc}(\gamma_2 d) \right\} \xi^2 \end{aligned} \quad (64)$$

where  $\text{sinc}(x) = \sin(x)/x$ .

To better observe the discontinuity at  $z = d$ , the region from  $z = 0.9d$  to  $z = 1.1d$  has been expanded in Fig. 7(A). We note also in expression (64) that the value of the discontinuity at the interface is proportional to the square of the chiral admittance  $\xi$ . This proportionality is confirmed from the fact that in Fig. 6(B) we had to zoom in a region one hundred times smaller than in Fig. 7(A). This was done in order to observe a similar discontinuity as the chiral admittance was ten times smaller.

On the other hand,  $\mathbf{B}_z$  is zero on the perfectly conducting surface and continuous on the chiral-free space interface, as shown in Fig. 7(B).

## 8. CONCLUSIONS

We have presented an alternative formulation for guided electromagnetic fields in grounded chiral slabs. This formulation is formally equivalent to the double Fourier transform method used by the authors to calculate the spectral fields in open chirostrip structures. Special attention to the behavior of the electromagnetic fields in the vicinity of the ground plane and on the interface between the chiral substrate and free space was given. It has been observed that, inside a chiral substrate and on the interface with a perfectly conducting surface, the magnetic field component normal to this surface is not null. Moreover, on the interface between a chiral substrate and free space, the magnetic field component normal to this interface is not continuous even when the magnetic permeability is the same in the two media. Clearly, chirostrip structures exhibit unusual boundary conditions for the magnetic field when compared with microstrip structures.

## ACKNOWLEDGMENTS

This work was supported, in part, by the Brazilian Research Council (CNP<sub>q</sub>), under Grant 521049/94-6.

## REFERENCES

1. Cory, H., "Chiral devices – an overview of canonical problems," *J. Electromagn. Waves Appl.*, Vol. 9, No. 5/6, 805–829, 1995.
2. Pelet, P., and N. Engheta, "Novel rotational characteristics of radiation patterns of chirostrip dipole antennas," *Microwave Opt. Technol. Lett.*, Vol. 5, No. 1, 31–34, January 1992.
3. Pelet, P., and N. Engheta, "Chirostrip antenna: line source problem," *J. Electromagn. Waves Appl.*, Vol. 6, No. 5/6, 771–793, 1992.
4. Pozar, D. M., "Microstrip antennas and arrays on chiral substrates," *IEEE Trans. Antennas Propagat.*, Vol. AP-40, No. 10, 1260–1263, October 1992.
5. Lumini, F., and J. C. S. Lacava, "A full-wave analysis method for open chirostrip structures," *Proceedings of the ICAP 1993*, Edinburgh, UK, 37–40, March/April 1993.
6. Pelet, P., and N. Engheta, "Mutual coupling in finite-length thin wire chirostrip antennas," *Microwave Opt. Technol. Lett.*, Vol. 6, No. 12, 671–675, September 1993.
7. Pelet, P., and N. Engheta, "Theoretical study of radiation properties of a finite-length thin-wire chirostrip antenna using dyadic Green's functions and method of moments," *Progress in Electromagnetics Research (PIER)*, Vol. 9 on Bianisotropic and Bi-isotropic Media and Applications, A. Priou (Ed.), EMW Publishing, Cambridge, Massachusetts, Chapter 14, 265–288, 1994.
8. Lacava, J. C. S., and F. Lumini, "Electromagnetic fields in open chirostrip structures excited by printed dipoles," *Proceedings of the 1995 IEEE AP-S/URSI International Symposium*, Newport Beach, California, USA, 52, June 1995.
9. Mariotte, F., P. Pelet and N. Engheta, "A review of recent study of guided waves in chiral media," *Progress in Electromagnetics Research (PIER)*, Vol. 9 on Bianisotropic and Bi-isotropic Media and Applications, A. Priou (Ed.), EMW Publishing, Cambridge, Massachusetts, Chapter 12, 311–350, 1994.
10. Engheta, N., and P. Pelet, "Surface waves in chiral layers," *Opt. Lett.*, Vol. 16, No. 10, 723–725, May 1991.

11. Paiva, C. R., and A. M. Barbosa, "A method for the analysis of biisotropic planar waveguides: application to a grounded chiroslabguide," *Electromagnetics*, Vol. 11, 209–221, 1991.
12. Lumini, F., and J. C. S. Lacava, "Radiation properties of chirostrip antennas," *Proceedings of the 1993 SBMO International Microwave Conference*, São Paulo, Brazil, Vol. 2, 587–592, August 1993.
13. Lumini, F., and J. C. S. Lacava, "Near field solutions for chirostrip printed dipoles," *Proceedings of the 1995 SBMO/IEEE MTT-S International Microwave and Optoelectronics Conference*, Rio de Janeiro, Brazil, Vol. 1, 253–258, July 1995.
14. Sihvola, A. H., and I. V. Lindell, "Bi-isotropic constitutive relations," *Microwave Opt. Technol. Lett.*, Vol. 4, No. 8, 295–297, July 1991.
15. Harrington, R. F., *Time-Harmonic Electromagnetic Fields*, McGraw-Hill Book Company, New York, 1961.
16. Ougier, S., I. Chenerie, and S. Bolioli, "Measurement method for chiral media," *Proceedings of the 22nd European Microwave Conference*, Espoo, Finland, Vol. 1, 682–687, August 1992.